SANDIA REPORT
SAND2023-05851
Printed June 2023

Sandia National Laboratories

Assessment of tank designs for hydrogen storage on heavy duty vehicles using metal hydrides

Mark D. Allendorf, Robert Horton, Vitalie Stavila, and Matthew Witman

Prepared by
Sandia National Laboratories

Issued by Sandia National Laboratories, operated for the United States Department of Energy by National Technology & Engineering Solutions of Sandia, LLC.

Available to DOE and DOE contractors from
U.S. Department of Energy
Office of Scientific and Technical Information
P.O. Box 62
Oak Ridge, TN 37831

Telephone: (865) 576-8401
Facsimile: (865) 576-5728
E-Mail: reports@osti.gov
Online ordering: http://www.osti.gov/scitech

Available to the public from
U.S. Department of Commerce
National Technical Information Service
5301 Shawnee Rd
Alexandria, VA 22312

Telephone: (800) 553-6847
Facsimile: (703) 605-6900
E-Mail: orders@ntis.gov
Online order: https://classic.ntis.gov/help/order-methods/

ABSTRACT

The objective of this project was to evaluate material-based hydrogen storage solutions as a replacement for high-pressure hydrogen gas or liquid hydrogen on Class 7 or 8 tractor fuel cell electric vehicles. The project focused on low-density main-group hydrides, a well-known class of materials for hydrogen storage. Prior research has considered metal amides as storage materials for light-duty vehicles but not for heavy-duty applications. The project established the basis for further development of storage systems of this type for heavy duty vehicles (HDV). Systems analysis of an HDV storage system comprised of a tank and associated balance of plant (piping, coolant tubes, burner) was performed to determine the usable hydrogen capacity. A composite storage material comprised of a metal hydride mixed with a high thermal-conductivity carbon is predicted to have a usable hydrogen volumetric capacity comparable to or exceeding that of 700 bar pressurized hydrogen gas. The gravimetric capacity of this material is also predicted to be competitive with pressurized gas, particularly if costly carbon fiber composite Type III or Type IV tanks are excluded. The storage system design parameters and material properties served as inputs to a second model that simulates fuel cell operation in conjunction with the storage system during an HDV drive cycle. The results show that sufficient hydrogen pressure can be produced to operate a Class 8 HDV, yielding a range of ~480 miles. These results are particularly relevant for high-impact regions, such as the South Coast Air Quality Management District, for which an economical vehicular hydrogen storage system with minimal impact on cargo capacity could accelerate adoption of heavy-duty fuel cell electric vehicles. An additional benefit is that knowledge generated by this project can assist in development of material-based storage for stationary applications such as microgrids and backup power for data centers.

ACKNOWLEDGEMENTS

The authors are grateful to Southern California Gas Company for the financial support of this project, and particularly to Project Managers Michael Lee and Jeffrey Chase for their technical and programmatic support. MA, VS, and MW would also like to thank Kriston Brooks (Pacific Northwest National Laboratory) for technical discussions and assistance associated with the system modeling, and Robert Horton and Walter Ramirez for characterization measurements of hydrogen storage materials. Sandia National Laboratories is a multi-mission laboratory managed by National Technology and Engineering Solutions of Sandia, LLC, a wholly owned subsidiary of Honeywell International Inc., for the DOE's National Nuclear Security Administration under contract DE-NA0003525. Studies at the Molecular Foundry of the Lawrence Berkeley National Laboratory were supported by the Office of Science, Office of Basic Energy Sciences, of the U.S. Department of Energy under Contract No. DE-AC02-05CH11231. The views and opinions of the authors expressed herein do not necessarily state or reflect those of the United States Government or any agency thereof. Neither the United States Government nor any agency thereof, nor any of their employees, makes any warranty, expressed or implied, or assumes any legal liability or responsibility for the accuracy, completeness, or usefulness of any information, apparatus, product, or process disclosed, or represents that its use would not infringe privately owned rights.

Table of Contents

This page left blank

Assessment of tank designs for hydrogen storage on heavy duty vehicles using metal hydrides

SoCalGas Research, Development, and Demonstration Program

Applicable Subprogram and Project Area: Clean Transportation On-Board Storage.

Principal Investigator/project lead: Dr. Mark D. Allendorf, Sandia National Laboratories
Mail Stop 9161, Livermore, CA 9455-0969
Phone: (925)294-2895
Email: mdallen@sandia.gov

Project team: Robert Horton
Vitalie Stavila
Matthew Witman

ACRONYMS AND TERMS

Term	Definition
BOP	Balance of plant
DOE	Department of Energy
DSC	Differential scanning calorimetry
ENG	Expanded natural graphite
FCEV	Fuel cell electric vehicle
FEA	Finite element analysis
FEM	Finite element modeling
HDV	Heavy duty vehicle
HHDDT	Heavy Heavy-Duty Diesel Truck
HSECoE	Hydrogen Storage Engineering Center of Excellence
HyMARC	Hydrogen Materials Advanced Research Consortium
LDV	Light duty vehicle
LOHC	Liquid organic hydrogen carrier
MDV	Medium duty vehicle
MOF	Metal-Organic Framework
MHSDT	Metal Hydride Storage Design Tool
MH	Metal hydride
PCT	Pressure-composition-temperature
TCR	Temperature coefficient of resistance
TEA	Techno-economic analysis
TSP	Transient plant source

1. BACKGROUND

1.1. On-board vehicular hydrogen storage

A major barrier to the use of hydrogen as a transportation fuel is its volumetric energy density (Figure 1), which is 27 g H_2 L^{-1} at the 700-bar (70 MPa) pressure used in commercially available fuel cell electric vehicles. This falls short of the 50 g H_2/L ultimate target set by the U.S. Department of Energy (DOE) for light duty vehicles.[1] Although cryo-compressed hydrogen is higher (44 g H_2 L^{-1}), it is uneconomical for some applications.[2] The economics of storage using liquid hydrogen includes a significant energy penalty associated with liquefaction (~30%),[3] as well as the need for cryogenic storage, thereby limiting the application space for this storage mode. Consequently, storage of hydrogen using solid-state materials, such as nanoporous sorbents and metal hydrides, continue to attract considerable interest. The objective of this project is to evaluate metal hydride composites as a materials-based storage medium to replace high-pressure hydrogen gas on Class 7 or 8 tractor fuel cell electric vehicles (FCEV).

For heavy duty vehicles (HDV), current proposed designs for Class 8 tractors use compressed gas technology to store hydrogen. The amount of hydrogen stored in such tanks is ~55 kg, but containment at these pressures requires a steel tank weighing >9240 kg (4200 lbs) vs. 330 kg (150 lbs) for diesel fuel. The combined weight of the fuel storage system, including the tank, fuel, and ancillary "balance of plant" such as piping, can reduce the cargo capacity by as much as 10%. Although high-pressure hydrogen gas is cost-competitive with batteries, the gas storage system is still a major contributor to the high cost of these vehicles, adding as much as $50,000 to the cost of a CNG-fueled truck compared with a diesel truck.[4] In contrast, many material-based alternatives have volumetric energy densities higher than even liquid hydrogen, but lower gravimetric energy densities (Figure 1).

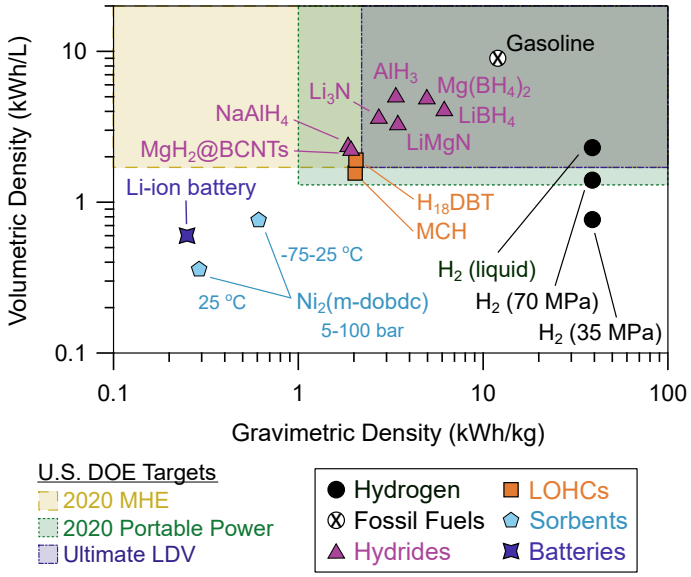

Figure 1. Comparison of the volumetric and gravimetric energy densities of hydrogen storage materials with US DOE technical targets.[5]

1.2. Metal Hydrides as a replacement for high-pressure hydrogen gas storage

Metal hydrides (MH) are one of three major categories of hydrogen storage materials under consideration worldwide, the others being nanoporous sorbents and liquid organic hydrogen carriers (LOHC). Extensive research focused on developing these materials for transportation and other applications has been conducted, accelerating considerably after it was shown that the complex hydride $NaAlH_4$ could be made reversible by using additives such as titanium halides.[6] Metal hydride materials have several important advantages for on-board hydrogen storage:

- The volumetric capacity of many metal hydrides is higher than 700 bar compressed gas and can even exceed that of liquid hydrogen (Figure 1).[5]
- The equilibrium pressure above a hydride storage bed while delivering H_2 to a fuel cell is far lower than that used in high-pressure gas storage tanks (350 bar or 700 bar), reducing both safety concerns and infrastructure costs. Moreover, H_2 release from metal hydrides is thermally activated and can be tailored to match the requirements of the fuel cell. Thermal activation could be achieved, for example, using residual heat released by the proton exchange membrane (PEM) fuel cell to increase the overall energy efficiency.
- Depending on the thermodynamics and kinetics of the particular hydride, full regeneration is possible following H_2 desorption, using pressures much lower than 700 bar. For example, the metal amides considered in this project can be regenerated under 100 bar hydrogen.[7] Consequently, on-board storage tanks designed to withstand ultrahigh pressures, which are heavy and expensive, are not needed. Moreover, at these much lower pressures, low-cost compressors can be used, which reduces the cost of the fueling infrastructure.
- Many hydrides are comprised of light, earth-abundant elements, such as Li, B, N, Na, Mg, and Al. This makes them attractive for transportation applications due to their high gravimetric energy storage capacity, which can be an order of magnitude or more greater than batteries (Figure 1).[5]

1.3. Sandia-developed metal amide composites

Metal amides and imides are attractive candidates for material-based storage systems because of their high gravimetric and volumetric capacities, promising thermodynamics, and reversibility.[7] For example, the lithium amide/lithium hydride system ($LiNH_2$+LiH) has a reversible gravimetric capacity of 6.5 wt% H and $\Delta H_{des} = 45$ kJ/mol H_2.[8] However, the material is unusable in bulk form for PEM fuel cells because the combination of slow H_2 desorption kinetics and heat transport at practical bed operating temperatures makes the hydrogen release rate too low to allow a fuel cell to operate. This material also releases ammonia upon hydrogen release, which degrades the storage capacity. The Sandia HyMARC team developed two strategies to address this problem—nanoscaling and hydride-carbon composites—that demonstrate that the poor kinetics and heat transport of the bulk material can be manipulated to achieve properties required for materials-based hydrogen storage.

1.3.1. Nanoscaling for improved kinetics and heat transport

Initial efforts in HyMARC to address the heat transport problem focused on a nanoscaling strategy previously developed in which Li_3N was synthesized within a porous carbon host and then hydrogenated to create the storage material, $LiNH_2/2LiH$. In this concept, the host performs several functions. First, its high thermal conductivity accelerates the H_2 release reaction throughout the tank. Second, confinement within the nanoscale pores (3 – 6 nm diameter; Figure 2) of the host destabilizes the hydride, allowing it to release H_2 at 150 °C lower than the bulk material.[9] This also enables the material to be fully reversible at 100 bar H_2 (Figure 3), with uptake of ≈ 5 wt% H relative to the mass of the sample, i.e., including the mass of the inert carbon scaffold. This translates to the active material cycling reversibly at ≈ 10.3 wt% H, consistent with the theoretical capacity of complete interconversion between [$LiNH_2$ + 2LiH] and Li_3N. Third, the host allows the addition small quantities (~1 mol%) of other hydrides to improve the desorption and rehydrogenation kinetics; this can nearly triple the H_2 release rate, reducing the required bed temperature and with it the balance of plant required to deliver the gas to the fuel cell. Finally, the Sandia-patented method used to infiltrate Li_3N into the pores[10] improves the safety of the synthetic process by employing less reactive nitrogen starting material. We demonstrated this approach for carbon porous carbons with pore sizes ranging from 0.95 to 12.3 nm (Figure 2).

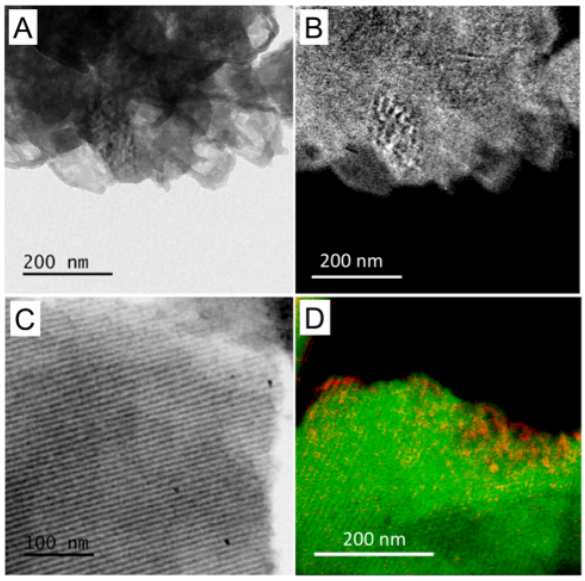

Figure 2. Li_3N infiltration in nanoporous carbons. **A.** TEM image of 6 nm porous carbon with a random pore geometry/orientation. **B.** EFTEM Li map showing homogeneous Li_3N distribution within the pore. **C.** TEM image of a templated CMK-3 carbon with pore sizes of 5 nm. **D.** EELS maps of Li (orange) showing Li_3N incorporation into 5 nm ordered carbon (green) pores.

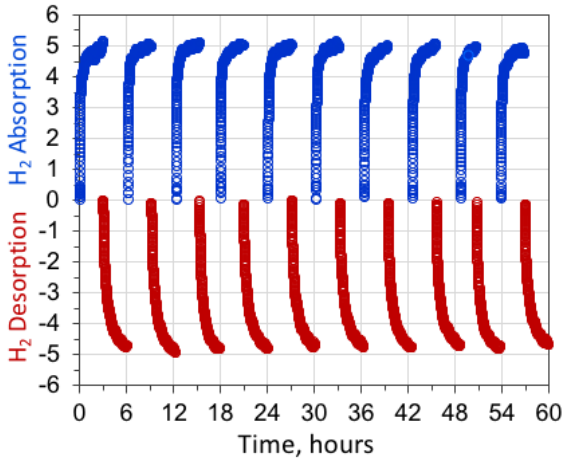

Figure 3. Reversible hydrogen uptake and release in Li_3N@6nm-carbon over 10 cycles of hydrogen absorption and desorption.

Ternary amides (e.g. Li-Mg-N-H) are a more attractive option than $LiNH_2$+LiH because of their more favorable hydrogen release thermodynamics while maintaining relatively high hydrogen capacity. For example, the mixture 2:1 LiH:$Mg(NH_2)_2$, which displays more favorable thermodynamics (ΔH_{des} = 39 kJ/mol H_2 and ΔS_{des} = 112 J/mol H_2 K),[11, 12] and a relatively high reversible hydrogen storage capacity (5.0 wt. %). Unfortunately, although the nanoscaling strategy is successful for $LiNH_2$+LiH, we discovered during the project that creating nanoscale mixed-metal amides such as 2:1 LiH:$Mg(NH_2)_2$ is quite difficult. In particular, it proved difficult to achieve a loading sufficient to obtain the necessary stoage capacity. Consequently, for the remainder of the project we focused on using Li-Mg amides in their pure form or as a composite mixture with another material to enhance its thermal conductivity (see below).

1.3.2. *Hydride-carbon composites*

The thermal conductivity (k) of metal hydrides is generally poor, typically $\leq$ 1 W/m•K, and can be a strong function of the gas composition.[13] Engineering strategies to circumvent this problem have been developed and generally involve preparing a composite in which the hydride is mixed with a material with high thermal conductivity, such as graphite. For example, Sandia partnered with GM to develop a pilot-scale metal hydride storage tank, using sodium alanate ($NaAlH_4$) mixed with expanded natural graphite (ENG) at 10% mass loading.[14] ENG is prepared through acid treatment and heating of nature graphite to generate fine flakes. Hydride-ENG composites having ten-fold higher k than bulk have been reported.

1.4. Project Description and Approach

1.4.1. Project objective and potential benefits

The aim of this project was to evaluate the potential of metal hydrides as replacements for pressurized hydrogen gas storage for FCEV Class 8 tractors. A secondary goal was to establish the basis for further development of storage systems of this type for HDV. The results are particularly relevant for high-impact regions, such as the South Coast Air Quality Management District, for which an economical vehicular hydrogen storage system with minimal impact on cargo capacity could accelerate adoption of HD-FCEV. A side benefit is that knowledge generated by this project could assist in development

of material-based storage for stationary applications such as microgrids and backup power for data centers.

1.4.2. Project structure

The project was comprised of three tasks. Task 1 provided material property data for $2LiH:Mg(NH_2)_2$ needed to perform storage system modeling in Task 2. The objective of the storage system modeling in Task 2 was to determine whether a metal hydride could store sufficient usable hydrogen onboard the vehicle to yield an acceptable operating range (i.e., miles driven) within constraints imposed by available space for a storage system. The performance of several tank materials was assessed. In Task 3, outreach activities were conducted to share the results with the scientific and industrial community focused on fuel cell vehicles and renewable fuels.

2. RESULTS

2.1. Task 1 – Hydride materials synthesis and characterization

2.1.1. Material selection

The metal hydride considered for this investigation was 2:1 lithium hydride:magnesium amide ($2LiH:Mg(NH_2)_2$) due to its favorable thermodynamics and storage capacity, as discussed above.[7] This hydride has been considered as a storage material for LDV[15] but not for HDV applications. Experiments suggest that its thermodynamic properties (specifically, the enthalpy of H_2 desorption) are intermediate between lithium amide and magnesium amide ($Mg(NH_2)_2$).[16-18] Although the thermodynamics of bulk $Mg(NH_2)_2$ are well-suited to vehicular storage, desorption is not reversible due to release of ammonia during decomposition, making it unsuitable as an energy carrier for HDV. In contrast, LiH does not decompose until very high temperatures due to its large $\Delta H_{des} = 181$ kJ/mol H_2.[19]

Although the properties of $2LiH:Mg(NH_2)_2$ have been previously reported, our experience is that literature values of key material properties needed for systems modeling are not always accurate. For example, the equilibrium H_2 pressure above the hydride can be inaccurate if the time allotted for the Pressure-Composition-Temperature (PCT) measurement was not sufficient for the materials to reach equilibrium. Consequently, in this task we performed a series of measurements designed to obtain reliable data for Task 2 modeling:

2.1.2. Hydride synthesis and characterization

Li-Mg amides can be synthesized using a variety of starting materials, including LiH, $LiNH_2$, MgH_2, and $Mg(NH_2)_2$. A mixture of $Mg(NH_2)_2$ and LiH is equivalent to the $2LiNH_2 + MgH_2$ system because the two hydride-amide pairs undergo a metathesis reaction:[7]

$$2LiNH_2 + MgH_2 \leftrightarrow Mg(NH_2)_2 + 2LiH \quad (1)$$

In this project, we prepared the Li-Mg amide by ball-milling $LiNH_2$ and MgH_2 in a 2:1 molar ratio. This material decomposes according to reaction (2):

$$Mg(NH_2)_2 + 2LiH \leftrightarrow Li_2Mg(NH)_2 + 2H_2 \quad (2)$$

yielding a theoretical gravimetric capacity of 5.6 wt%. Synthesis and handling of air-sensitive materials were carried out under an Ar atmosphere in a glove box.

However, it is known from the literature[7, 20] as well as our own work that addition of certain metal hydrides, such as LiH, KH, and KBH_4, can increase the gravimetric capacity, improve the reversibility, and accelerate H_2 release. HyMARC is conducting experiments to determine which quantities of additive(s) provide the best compromise among the various properties of the material. For the scope of this project, we elected to focus on a single metal hydride composition, ($2LiNH_2$:$1MgH_2$:0.1KH:0.1LiH; referred to in this report as the 2:1 material) as it is known that small amounts of KH improve the desorption kinetics and reversibility.[20] This is a reversible material with fast dehydrogenation kinetics and adequate thermodynamic properties to operate a fuel cell. The ($2LiNH_2$: $1MgH_2$: 0.1KH : 0.1LiH) composite was synthesized by ball-milling the four reactant hydrides for 120 minutes in a stainless steel vessel lined with tungsten carbide.

Table 1. The intrinsic properties of ($2LiNH_2$:$1MgH_2$:01KH:0.1LiH).

Description	Value	Units
Theoretical hydrogen gravimetric capacity	6.70[a]	percent
Enthalpy of desorption per mol H_2 (ΔH)	40400	J/mol
Entropy of desorption per mol (ΔS)	114	J/mol•K
Thermal conductivty[d] (κ)	0.27 (25 °C) 0.43 (250 °C)	W/m•K
Crystalline density of metal hydride	1090	kg/m^3
Heat capacity, 298 K	75.25[b]	J/mol•K
Surface area	0[c]	m^2/g
Desorption rate (Eqn. 2): preexponential (A)	2.31E+10	s^{-1}
Desorption rate (Eqn. 2): activation energy (E)	126.5	kJ/mol
Desorption rate (Eqn. 2): reaction order (n)	1.17	unitless

[a] Assumes complete decomposition to Li_3N, Mg, K, and Li. [b]Assumed to be the same as Li_3N as reported in Ref. [21]. [c] This is a bulk material and has no intrinsic porosity. [d]Under 1 bar H_2.

2.1.3. Hydride thermodynamics and H_2 release kinetics

Our PCT instrument can measure these properties under pressures as high as 200 bar and is equipped with a mass spectrometer to monitor the purity of the evolved gas. A high-pressure differential scanning calorimeter (DSC) instrument is also connected to the instrument and is used to determine the thermodynamics of phase changes that occur during H_2 release and uptake. These data were obtained using best practices determined by the hydrogen storage community.[22]

The Sieverts apparatus (Figure 4) measures hydrogen absorption or desorption at carefully controlled temperature, pressure, and timing, yielding a so-called PCT curve (pressure-composition-temperature). The basic operation is to measure the change in pressure when a material is exposed to a suddenly increased or decreased hydrogen pressure. Careful accounting must be made for reservoir and source volumes, since the fractional absorption by the material is often small. Results are typically expressed as the percentage, by weight, of hydrogen absorbed or released by a material. Values range from fractions of 1% up to about 15% H by weight. Time scales vary from minutes to days.

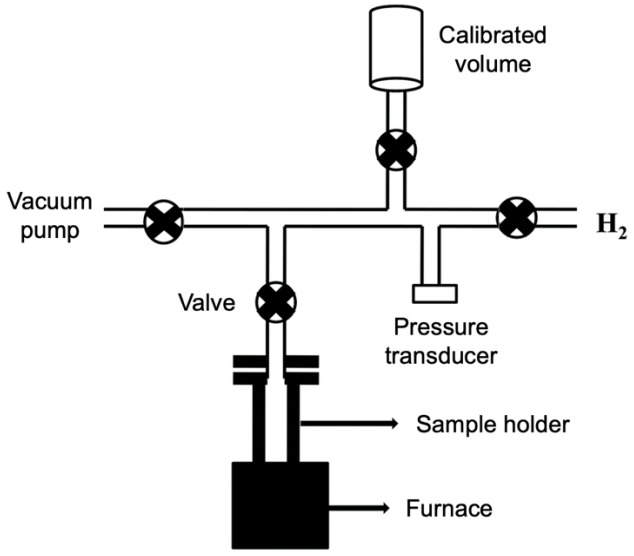

Figure 4. Schematic of the Sieverts apparatus used to measure the thermodynamic properties and rate of H_2 release of metal hydrides

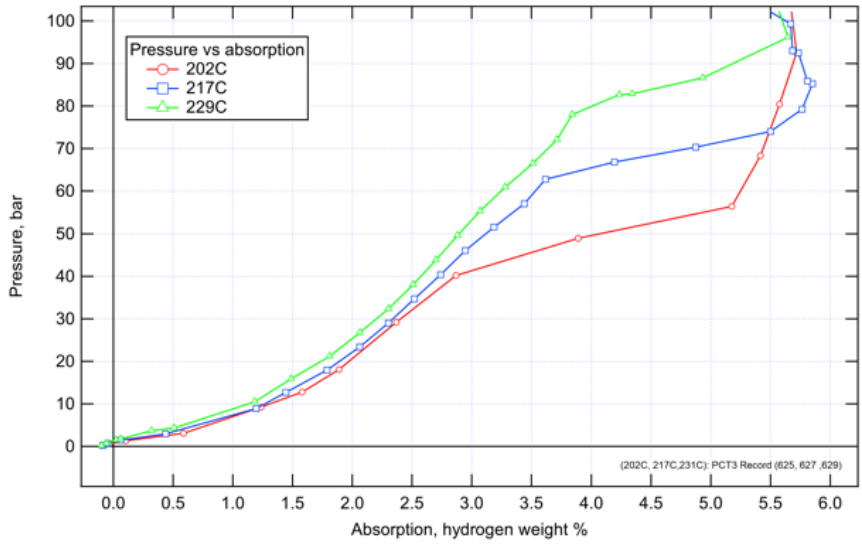

Figure 5. Representative PCT curves for 2:1 LiH:$Mg(NH_2)_2$. A mixture of KH and LiH hydrides was added, which improves cyclability and hydrogen release kinetics.

A typical set of PCT curves for the 2:1 material is shown in Figure 5. Thermodynamic values are extracted from such data using the Van't Hoff equation (Equation 1) and the results are given in Figure 6 and Table 1. The values of ΔH and ΔS are in reasonable agreement with values in the literature,[7] although these vary depending on the particular additives used and their amounts (the composition considered for this project has not been previously reported).

$$\ln K = -\frac{\Delta H^o}{R}\frac{1}{T} + \frac{\Delta S^o}{R} \tag{1}$$

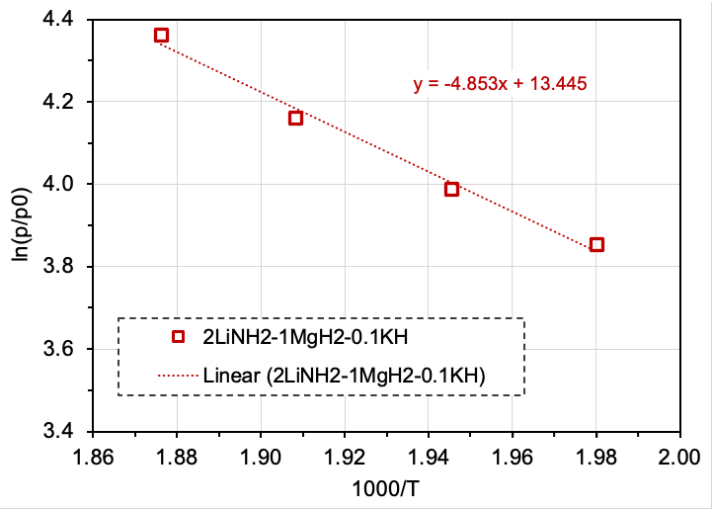

Figure 6. Van't Hoff plot of PCT data obtained for the metal hydride 2:1 LiH:$Mg(NH_2)_2$.

The rate of hydrogen desorption from the material was obtained from Sieverts apparatus data (Figure 7) and analyzed using Equation (2):

$$\partial X/\partial t = Aexp(-E/RT)(1-X)^n \tag{2}$$

where X is the fractional conversion, A is the pre-exponential factor, E is the activation energy, and n is the reaction order. Values of A and E are given in Table 1; these describe the global desorption kinetics occurring in the Sieverts experiment, which may include processes other than the chemical reaction (e.g., mass transport). The data were obtained within the temperature regime considered in the modeling described below and are thus assumed to be representative of the processes occurring when hydrogen is released from the amide in the fuel tank. The activation energy is consistent with our previous work on other complex hydrides, in particular $NaAlH_4$.[23]

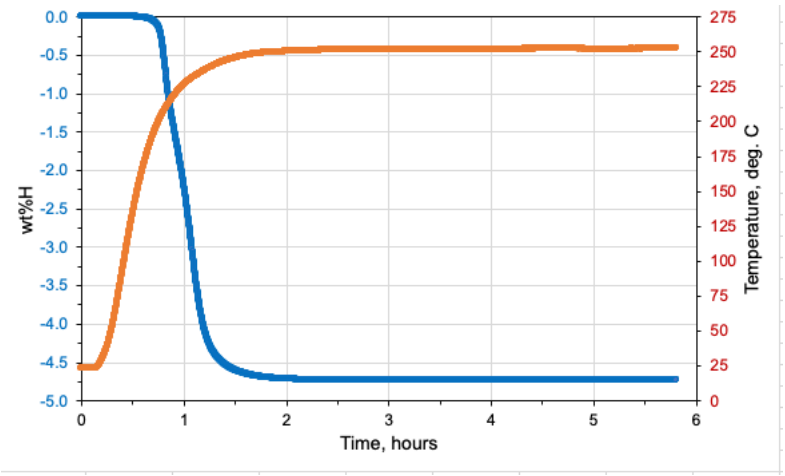

Figure 7. Rate of H_2 release from ($2LiNH_2$:$1MgH_2$:0.1KH:0.1LiH) measured using a Sieverts apparatus. Orange curve: sample temperature as a function of time. Blue curve: corresponding amount of H_2 released, given as the weight percent of the sample.

2.1.4. Heat transfer rates

The thermal conductivity κ of amide samples was measured using a commercial instrument using the transient plant source (TSP) technique. Samples are contained within a controlled-atmosphere chamber, allowing us to conduct measurements in both inert gas (typically argon) and hydrogen. A nickel coil with a known temperature coefficient of resistance (TCR) is heated between two homogenous samples (Figure 8). Samples consisted of pellets prepared in a press in an argon glove box using 10,000 psi. The instrument measures the resistance of a nickel coil during a transient heat wave, yielding sample temperature as a function of time (Figure 8).

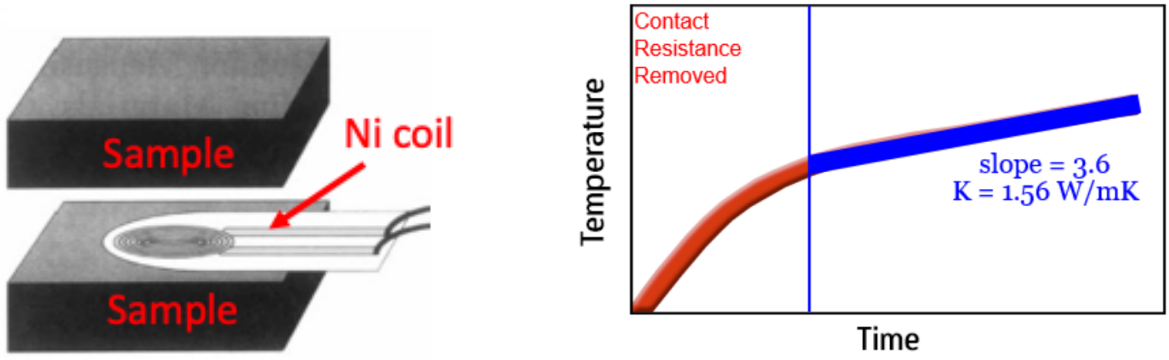

Figure 8. Schematic of the apparatus used to measure the heat transport rate of a metal hydride (left) and typical data (right).

The thermal conductivity varies considerably depending upon the morphology of the material (powder or pressed pellet) and whether or not the metal hydride is mixed with thermally conducting carbon. As seen in Figure 9, bulk hydride powders have low thermal conductivity, less than 0.5 W m^{-1} K^{-1}). In general, the thermal conductivity increases with temperature; this is beneficial for using them as storage materials because temperatures above ambient are needed to drive the desorption reaction. The addition of small amounts (1 wt%) of a conductive carbon has no beneficial effect, but adding up to 10 wt% produces a measureable increase. What is clear (and not surprising), however, is that the thermal contact with a powder is poor. However, pressing the hydride/carbon mixture into a pellet makes a dramatic improvement in κ, increasing the value by nearly a factor of 20 over pure bulk metal hydride powder (4.8 W/m/K vs. 0.27 W/m/K). This is beneficial not only from the perspective of improved heat management but also because material handling of pellets is easier than for powders. For the purposes of the system modeling done here, we assumed a value of 3.8 W m^{-1} K^{-1} for the ($2LiNH_2$:$1MgH_2$:0.1KH:0.1LiH) composite with 10 wt% expanded graphite (Table 1) manufactured by SGL (Wackersdorf, Germany). Although higher amounts of this carbon yield a higher thermal conductivity, this also reduces the capacity (gravimetric and volumetric) of the material because the carbon absorbs no hydrogen. Future work by HyMARC will focus on achieving the optimum balance between thermal conductivity and capacity.

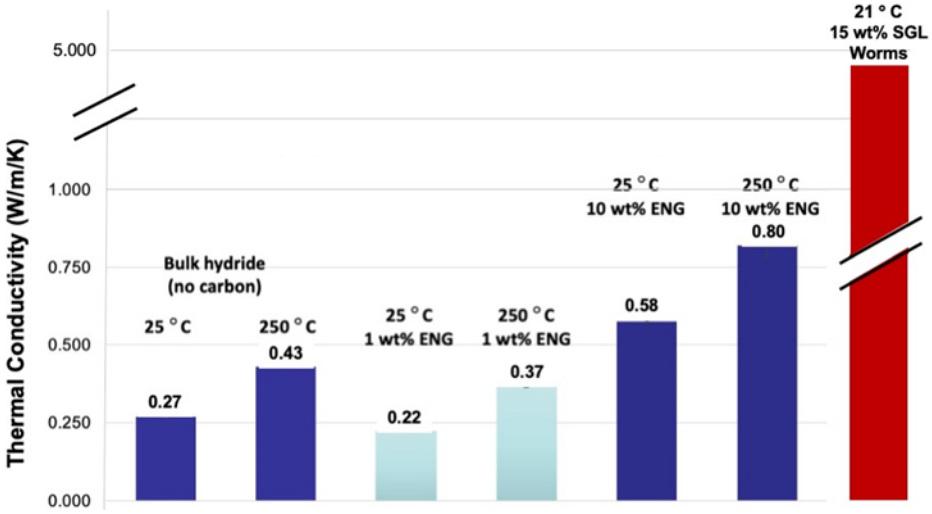

Figure 9. Thermal conductivity of ($2LiNH_2$:$1MgH_2$:0.01KH) powders (dark and light blue), in pure form and mixed with engineered graphite (ENG) and SGL expanded graphite. Pressing these powders into pellets (red) increases the thermal conductivity by a factor of 2-3 depending on the pressure used to form the pellet.

2.2. Task 2 – Tank modeling

2.2.1. Description of the model

The tank modeling performed in this study employed two codes. First, the Hydrogen Storage Tank Mass and Cost Estimation Model, or "Tankinator" model,[24-26] developed as part of the DOE Hydrogen Storage Engineering Center of Excellence (HSECoE), was originally developed for LDV

and was used here to model tanks designed to hold high-pressure hydrogen gas.[27,28] The Metal Hydride Storage Design Tool (MHSDT)[29] was used to cross-compare various pressure vessel types by estimating gravimetric, volumetric, and cost performance of hypothetical tanks in the conceptual phases of design (Figure 10). The model is a MATLAB version of the Tankinator code that, in conjunction with HyMARC and in response to the needs of this SoCalGas project, was created to consider metal hydrides and LDV, MDV, and HDV. In particular, it allows for multiple tanks that store a much greater quantity of hydrogen (60 kg for HDV vs. 5 kg for the LDV version). The HyMARC PNNL team (led by Kriston Brooks) developed this computational tool for estimating the mass and material composition for cylindrical Type I (various steel and aluminum alloys), Type III (composite with Al liner), and Type IV (composite with plastic liner) hydrogen storage tanks in a Microsoft Excel format. The number of tank fabrication materials that can be considered was also expanded to include twelve steel and aluminum alloys as well as the composite Type III and Type IV tanks. Scripts were also developed to automate MHSDT to assess the sensitivity of model predictions to various intrinsic material properties.

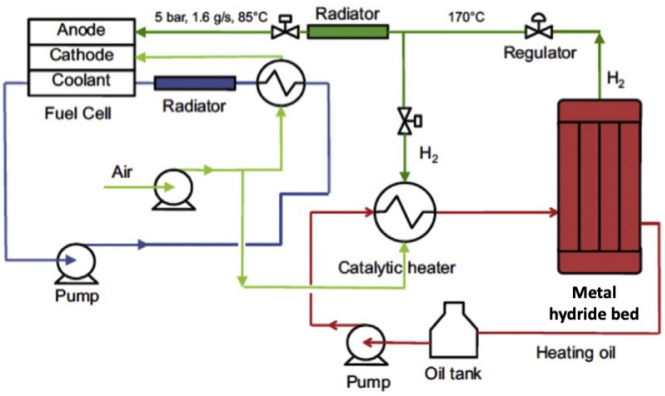

Figure 10. System flow chart in the MHSDT for a complex metal hydride such as $NaAlH_4$ (adapted from Ref. [29]).

The Tankinator and MHSDT tools provides an estimate of the mass and volume of the storage system, including the basic tank geometry and fabrication material from a limited number of geometric and temperature inputs. MHSDT also uses metal hydride physical properties to estimate the size of the entire storage system, including the metal hydride, heat exchanger, combustor, cooling tubes, and other balance of plant components. Heat transfer properties are used primarily to determine the number of cooling tubes required during refueling, which is an exothermic process. The MHSDT estimates the necessary vessel wall thickness for a given tank (specifying either diameter, length, or volume). The wall thickness of the cylindrical portion of the tank is primarily based on classic thin-walled pressure vessel hoop stress formula. End cap geometry is assumed to be perfectly hemispherical with wall thicknesses equal to the cylindrical section. Although MHSDT is only an estimation tool, its accuracy has been verified using finite element analysis (FEA) showing that the wall thicknesses predicted by the estimation tool results in an acceptable stress state. Additional details regarding the design properties associated with the four tank types and the assumptions incorporated into the metal hydride preprocessor can be found in Ref. [25].

2.2.2. *Inadequacy of pressurized gas as a storage medium for HDV*

The Tankinator model can be used to design a pressurized gas storage system and to determine the sensitivity of the results to the tank material. The results obtained from these calculations serve as benchmarks for material-based storage solutions. A comparison of the system gravimetric and volumetric capacities achieved for compressed gas (350 bar or 700 bar) for several tank materials is shown in Figure 11 and Appendix 1. These simulations reveal the obvious advantage of using lighter materials than 316 stainless steel to increase the volumetric capacity of a pressurized gas system. Note that although the volumetric capacity of a 700-bar tank is higher than that of a 350-bar tank, the added mass required to hold the higher pressure significantly reduces the gravimetric capacity. Additional comparisons with the metal amide material are discussed below.

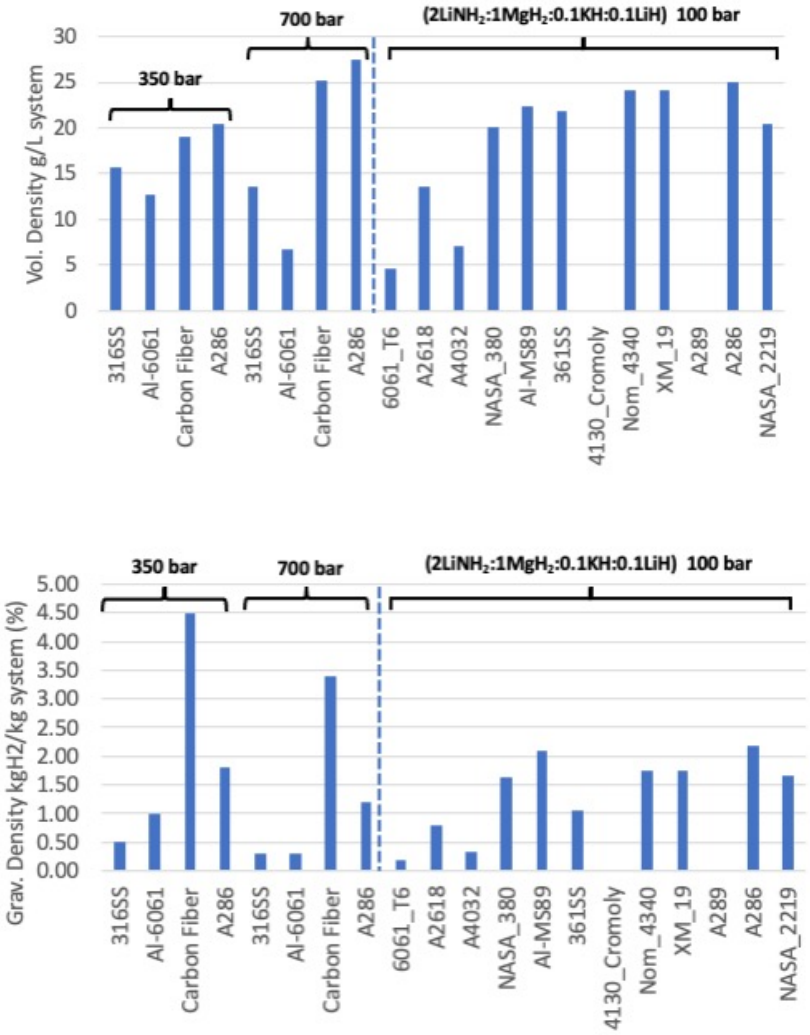

Figure 11. Comparison of volumetric and gravimetric hydrogen capacities for 350 bar and 700 bar compressed gas and the metal amide ($2LiNH_2$:$1MgH_2$:0.01KH) system predicted by the MHSDT model. Capacities are computed for several tank materials. For two of these materials, 4130_Cromoly and A289, the bed temperature required to produce the minimum-required hydrogen vapor pressure (5 bar) exceeds the limit of the material. For the amide, the maximum tank pressure is fixed at 100 bar. The carbon fiber results correspond to a Type III tank.

The mass of the system to store 60 kg of H_2 at 700 bar can be reduced by more than a factor of four relative to a conventional 316 stainless steel tank (Appendix 1). For example, the mass of a 316SS tank is predicted to be 23404 kg, whereas a tank fabricated from A286 steel, a high-strength Inconel-type alloy, would be 5068 kg. The lightest tank is a Type 4[30] carbon fiber laminate design, which has a mass of 1766 kg, but is undesirable due to its high cost. The results also can be compared with the DOE LDV volumetric and gravimetric targets, showing that, regardless of the tank material used, pressurized gas at 700 bar never exceeds 70% of the LDV volumetric target or 65% of the gravimetric target (Appendix 1). Although analogous targets are not available for HDV, we find that the MHSDT capacity predictions for HDV and LDV in absolute terms differ by <5% from each other (Table 2).

2.2.3. Tank design modeling for HDV

For the purposes of this investigation, we placed higher priority on maximizing system volumetric capacity than system gravimetric capacity. Although the latter is a concern for HDV, minimizing the volume occupied by the storage system in a HDV is paramount because this maximizes the amount of space available for cargo. To evaluate this and make comparisons with conventional pressurized gas systems we performed systems analysis in collaboration with Dr. Kriston Brooks (Pacific Northwest National Laboratory) to determine the features of a metal hydride storage system using a realistic tank configuration for a Class 8 tractor. This is shown in Figure 12 and is a combination of saddle tanks and tanks behind the cab. Inputs for the calculation, which include experimental property data for the metal amide storage material and fuel system design parameters, are given in Tables 3 and 4, respectively. The design for the resulting storage system, which includes BOP components such as coolant tubes, combustor (discussed below), ancillary tubing, and a tank fabricated from A286, are given in Table 5. Several key results related to volumetric capacity are summarized in Table 2.

The most important result of the systems analysis is that, assuming (2LiNH_2:1MgH_2:0.1KH:0.1LiH with 10 wt% SGL expanded graphite) as the storage material, the system volumetric hydrogen capacity of an A286 tank is equivalent to that of a costly carbon fiber tank operating at 700 bar. Two other alloys, Nom_4340 and XM_19, are similar, having a volumetric capacity 96% of 700 bar/carbon fiber (Figure 10). The comparison is also favorable on a gravimetric basis (Figure 11). If carbon fiber tanks are eliminated as a possible tank design for economic reasons (both for the cost of the tank itself and for a 700-bar compressor), the capacity of either an A286 or Al-MS89 metal hydride tank equals or exceeds that of an A286 tank at 700 bar. Critically, the maximum operating pressure of the metal hydride tanks is only 100 bar, which we expect will significantly reduce fueling station costs relative to 700 bar pressurized gas.

Several features of the storage system predicted by the MHSDT, listed in Table 5, should be noted. First, heat release during refueling is managed by coolant tubes inserted into the tank, the number of which is computed by the MHSDT. A greater number of tubes compared with pressurized gas is required for a metal hydride due to its large enthalpy of reaction. For the amide material considered here, 570 and 596 tubes are required for the saddle and rear tanks, respectively. Second, to achieve the minimum hydrogen pressure required on startup (5 bar), an on-board combustor is required that burns some of the available hydrogen (in this case 15.80 kg). Reducing the enthalpy of desorption could potentially eliminate the need for this, which reduces the storage capacity as well as adds weight. Finally, the total mass of the storage system is 2988 kg, though heavy compared with a Type 3 or Type 4 carbon fiber tank, this storage system nevertheless enables a 480-mile vehicle range, as discussed in the next section.

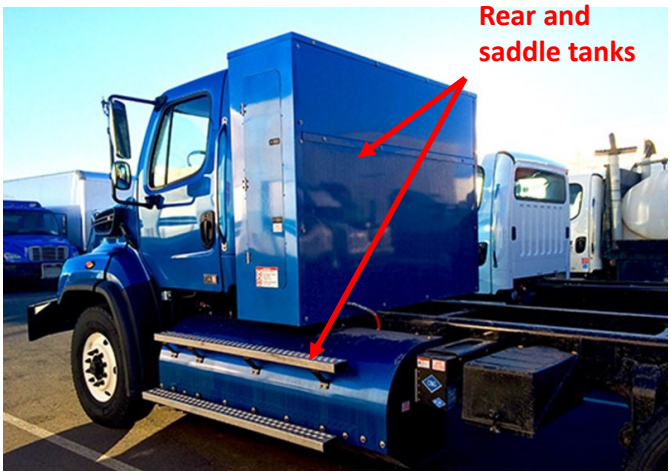

Figure 12. Tank configuration used in MHSDT and Vehicle Framework calculations.

Two aspects of the predicted tank design should be noted. First, heat must be supplied to the metal hydride bed to drive the decomposition reaction that releases H_2(g) (Reaction 2). This is accomplished using a burner that combusts some of the stored hydrogen; the combustion efficiency is set to be 80% (Table 4). Upon start up hydrogen to operate the burner is obtained from gas trapped within the void volume within the bed, which we assumed to be 30% of the total tank volume (Table 3). The mass of hydrogen required to maintain a minimum hydrogen vapor pressure of 5 bar (Table 4) is 15.8 kg (Table 5), leaving 44.2 kg hydrogen available to operate the fuel cell. Thus, the efficiency of stored hydrogen usage as 73.7% (this does not include the efficiency of the fuel cell).

Second, the maximum temperature of the hydride bed during operation is 260 °C (Table 5), which again is related to the temperature required to produce the minimum H_2 vapor pressure required to operate the fuel cell (assumed to be 5 bar). This result emphasizes the need for tank construction materials that are compatible with high temperatures. Although composite (Type III and IV) tanks have the advantage of being light-weight and can contain pressures up to 700 bar, their maximum operating temperature is only 85 °C.[31] It is important to note that this result applies only to ($2LiNH_2$:$1MgH_2$:0.1KH:0.1LiH/10 wt% SGL expanded graphite) hydride material. It is possible that other metal hydrides could be used that can produce the minimum 5 bar H_2 pressure at a lower bed operating temperature.

Table 2. Volumetric capacity of pressurized gas storage systems for LDV and HDV compared with the hydride-based storage system ($2LiNH_2$:$1MgH_2$:0.1KH:0.1LiH with 10 wt% SGL expanded graphite), as predicted by the Tankinator (pressurized gas) and MHSDT (hydride) models for selected tank materials of fabrication.

Storage system	g H_2/ L system (LDV)	g H_2/L system (HDV)
700 bar pressurized gas, Type I 316 stainless steel tank	14.4	13.5
700 bar pressurized gas, Type IV carbon fiber tank	25.5	25.1[b]
700 bar pressurized gas, Type I A286 tank[c]	28.0	27.5[b]
2:1 material, A286 tank[a]	23.0	25.0[a]
	2:1 amide, % of 700 bar	**2:1 amide as % of 700 bar**
Type IV carbon fiber tank	90%	93%
A286 tank	82%	85%

[a]2:1 amide material = ($2LiNH_2$:$1MgH_2$:0.1KH:0.1LiH) with 10 wt% SGL expanded graphite. Storage system for this material consists of two saddle tanks (d_o = 0.77 m, L = 2.02) and 1 rear tank (d_o = 0.79 m, L = 2.02 m). Maximum operating pressure is 100 bar. [b]Results courtesy of K. Brooks (PNNL). [c]Details of the input parameter values and outputs for the HDV case are given in Tables 3 – 5.

Table 3. Storage material properties used in MHSDT and Vehicle Framework Simulations for HDV.

Description	Value	Units
Hydride Carrying capacity of metal hydride	0.047[a]	decimal fraction
Fraction of inert in metal hydride bed (Enter 0 if f_H2 accounts for inert)	0	decimal fraction
Thermal Conductivty of hydride bed	3.85	W/m-K
Crystalline Density of metal hydride	1090	kg/m^3
Fraction of voids in metal hydride bed (Enter 0 if rho_cry = rho_bed)	0.3	decimal fraction
Density of inert material in hydride bed (Enter 0 if rho_cry = rho_bed)	0	kg/m^3
Enthalpy per mole H_2 rxn 1 (Endothermic +)	40400	J/mol
Entropy per mole H_2 rxn 1	114	J/mol-K
Enthalpy per mole H_2 rxn 2 (set to zero if single step rxn)	0	J/mol
Entropy per mole H_2 rxn 2 (set to zero if single step rxn)	0	J/mol-K
Moles H_2 produced per mole feed, Reaction 1 (Enter 0 if no rxn 2)	1	mol/mol
Moles H_2 produced per mole feed, Reaction 2 (Enter 0 if no rxn 2)	0	mol/mol

[a]For the composite mixture of metal hydride and SGL expanded graphite.

Table 4. Storage system parameters used in MHSDT and Vehicle Framework Simulations.

Description	Value	Units
Mass of useable H_2 available in the tank	60	kg
Coolant tube external radius	0.005	m
Coolant tube thickness	0.00089	m
Acceptable hydride temperature rise during refueling[a]	45	K
Upper hydrogen operating pressure	100	atm
Lower hydrogen operating pressure	5	atm
Hemispherical endcap option	Yes	
Tank material of construction	A286	
Maximum MH volume in 2 saddle tanks (2 m length, 0.65 m diam)	694	Liters
Maximum MH volume in rear tank (2 m length 0.75 m diam)	904	Liters
Target Refueling time (300 s = DOE LDV 2020 target)[b]	900	seconds
Combustion Efficiency (if required)	0.8	decimal fraction

[a]see Ref. [32] for a discussion of this parameter. [b]There is no target for HDV; we assume a longer refueling time due to the much larger quantity of usable hydrogen in the tank compared to a LDV.

Table 5. Storage system design and properties predicted by the MHSDT model.

Description	Value		Units
System mass	2988		kg
System volume	2.56		m^3
Combustor?	Yes		
Mass H_2 Burned	15.80		kg
	Saddle Tank	**Rear Tank**	
Number of Tanks	2	1	
Tank Outer Diameter	0.77	0.79	m
Tank Length	2.02	2.02	m
Number of coolant Tubes	570	596	
Tank Mass[a]	342	359	kg
Total Hydride Mass	1613		kg
Maximum Temperature	260		°C
Volume of Bed 1	0.69		m^3
Volume of Bed 2	0.73		m^3
Mass Hydride in Bed 1	530		kg
Mass Hydride in Bed 2	554		kg
Gravimetric density (g H_2/kg system)	20.1		
Volumetric hydrogen density (g H_2/L system)	23.4		
% of 700 bar systems using Carbon Fiber tank (= 25.1 g / L)	93		
% of 700 bar systems using A286 steel tank (= 27.5 g / L)	85		

[a]Mass of the tank, not including the hydride or other balance of plant components.

2.2.4. Sensitivity of MHSDT results to intrinsic material properties

Representative results of an automated series of screening calculations are shown in Figure 13 in the parameter space relevant to Li-Mg amides, using the MHSDT. For these calculations, a system configuration for a LDV was used and assumed a tank fabricated from A286 stainless steel, an iron-based superalloy. The objective of these calculations was to assess whether a hydride material can be designed that has a volumetric capacity >60% of the DOE 2025 Target,[1] i.e. better than 700 bar compressed H_2. We assumed a maximum tank operating pressure of 100 bar and varied ΔH, ΔS, and f_{H2} (the mass fraction of hydrogen in the storage material) for fixed values of the hydride bed density (kg/m^3) and thermal conductivity (W/m•K). In the 3D plots in Figure 13, blue dots represent theoretical materials for which the 60% target is not met and yellow dots indicate a combination of material properties that meet or exceed the target. Note that these calculations were performed by varying individual material properties (e.g. ΔH and ΔS) without consideration of whether a particular combination of properties is physically possible. Hence, the graphs enclosed in the red, green, and blue squares are highlighted, as these include values of κ and ρ that we know from experiments are feasible. Within each 3D plot of ΔH, ΔS, and f_{H2}, the values span values observed in various materials, with the caveat that correlations exist among these, such as entropy-enthalpy compensation (see discussion below), that may make some combinations unfeasible. Nevertheless, this screening investigation identified regions of property space that are promising for material development. As seen in the Figure 13, the properties for bulk lithium nitride (red box) and a nanoscale version of Li_3N (blue box) do not meet the target, primarily because of unfavorable thermodynamics (in particular, ΔH is too high). The region for a successful material is expanded in Figure 13 (right), which shows that increasing either the thermal conductivity and/or the bed density leads to regions of thermodynamic and f_{H2} space for which there are many material property combinations that will meet or exceed the target.

Encouragingly, the range of compositions that can meet the target is large. As long as κ is ≥1.1 W/ m•K and ρ is ≥750 kg/m^3, any combination of these yields a region of thermodynamic and mass fraction space with successful materials. Only modest increases in the thermal conductivity relative to bulk are required; a thermal conductivity of 1.1 W/ m•K is only slightly more than double that of the bulk material (Figure 9). The benefit of this large design space is that it opens the door to a number of strategies for achieving an optimal material. On the downside, however, it complicates the identification of structure-property relationships, as interdependencies among properties likely exist. One example is entropy-enthalpy compensation, in which a change to ΔH is partially counteracted by a change in ΔS. This mitigates the beneficial effect on the Gibbs free energy of reaction (ΔG). One way to address this problem is a machine learning strategy to identify Pareto-optimal materials, i.e., materials for which two or more competing objective properties cannot be simultaneously improved.[33] We demonstrated the effectiveness of this approach was demonstrated for high-entropy alloys (HEAs). We are currently assessing whether sufficient data exist to extend this model to hydrides such as the amides under consideration here.

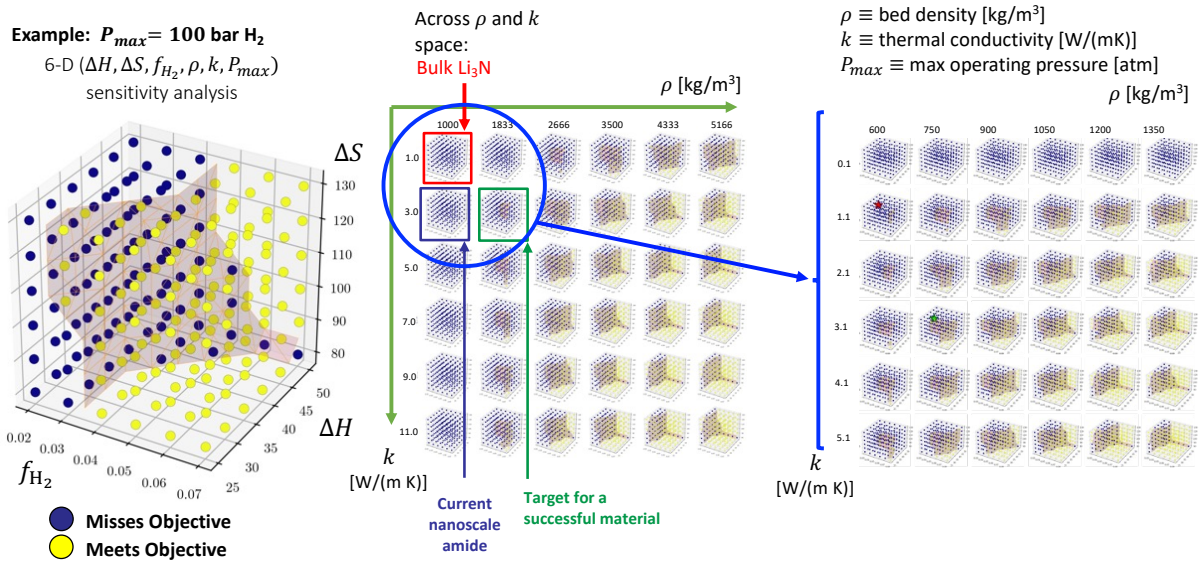

Figure 13. Matrix of MHSDT calculations for an A286 tank in which a maximum tank pressure of 100 bar is assumed and values of intrinsic material properties (Table 1) are varied. Blue dots represent combinations that do not exceed the volumetric capacity of 700 bar pressurized gas and yellow dots represents for which the material exceeds it. Red and blue boxes in the middle plot indicate the performance of the storage material bulk Li_3N and a nanoscale version of it. The green box, expanded in the right-hand figure indicates a region of potentially accessible properties for a hypothetical metal hydride.

2.2.5. Simulation of an integrated HDV fuel cell/metal hydride storage system

2.2.5.1. Vehicle Framework model description

The Hydrogen Vehicle Simulation Framework ("Framework model") is a MATLAB/Simulink tool for simulating a light-duty vehicle powered by a PEM fuel cell, which in turn is fueled by a hydrogen storage system. In conjunction with HyMARC and in response to this SoCalGas project, a version of the model was created that is applicable to HDV. The Framework model is designed so that the performance of different storage systems can be compared on a single vehicle, maintaining the vehicle and fuel cell system assumptions. There were minor changes made to the vehicle and fuel cell modules of the Framework Model to allow it to simulate a HDV. In addition to new drive cycles, it also required changing the characteristics of the vehicle (tire friction, wind resistance, vehicle weight, etc.) and the size of the fuel cell (maximum power). More significant changes were made to each of the storage modules compared with the LDV version. Rather than a single tank, the Framework-HDV allows multiple tanks, each operated in series. Hydrogen in the voids comes from all the tanks, but only a single tank is heated at a time and produces H_2 from the metal hydride to power the HDV.

The Framework Model is composed of a vehicle module, a fuel cell module, and a hydrogen storage module. The vehicle module computes demand for a given drive cycle. Power demand is based on acceleration, aerodynamic drag, rolling resistance, and component efficiencies. The drive cycles are repeated until some failure condition is encountered. This could be that the hydrogen has been depleted, the flow rate is insufficient, or some components are undersized for the vehicle's demand. The storage module uses the tank design obtained from the MHSDT model.

The responsibility of the fuel cell block is to translate power demand from the vehicle into hydrogen demand to the storage system. It also manages thermal balance and makes waste heat streams available for harvesting by the storage system. Note that this is not a fuel cell sizing tool: The performance curve is chosen to match DOE targets for efficiency (50% at rated power, 60% at 20% of rated power). The hydrogen storage system responds to hydrogen flow demands from the fuel cell system. It may also request auxiliary electrical power from the vehicle if needed, such as for heating and powering balance-of-plant components.

2.2.6. Framework HDV modeling results

To predict the operation of a fuel cell-powered HDV we used the fuel system parameters and material properties from the MHSDT model (Tables 3–5) as inputs to the Vehicle Framework model. The operation of the FC-HDV was simulated using the "6 HHDDT Cruise, 24C" drive cycle.[34] This is a cruise-mode segment chassis dynamometer test cycle for a heavy heavy-duty diesel truck and was developed by the California Air Resources Board (CARB) and West Virginia University. Features of the drive cycle are given in Table 6 and a plot of the speed vs. time is shown in Figure 14.

Table 6. Properties of the CARB Heavy Heavy-Duty Diesel Truck (HHDDT) Transient Segment drive cycle.[34]

Cycle	Time (minutes)	Distance (mi)	Maximum Speed (mph)	Average Speed (mph)	Average Driving Speed (mph)	Positive Kinetic Energy (ft/sec2)	Kinetic Intensity (1/mi)	Stops (#)
34.73	23.07	59.3	39.86	43.22	0.27	0.12	6	34.73

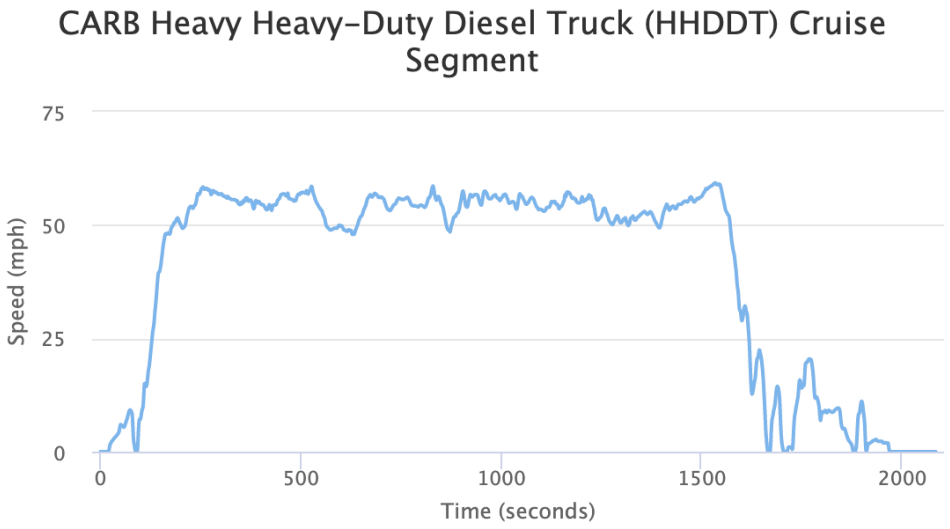

Figure 14. Speed vs. time profile for the HHDDT drive cycle used in the Vehicle Framework simulations (courtesy K. Brooks, Pacific Northwest National Laboratory).

Results of the simulation are shown in Figure 15. The curve in the figure plots the pressure in the fuel tank as a function of time. Because the fuel system is comprised of three tanks, there are large excursions in the pressure when one of the tanks is emptied. During start up or the transition from one tank to the next, the fuel cell continues to operate using residual hydrogen trapped in the porosity of the hydride material. This indicates that porosity must be a feature of the material in the fuel tank. The small oscillations in the flat regions of the plot are due to the drive cycle, which simulates operation of the vehicle as it travels through various terrain (for example, climbing a hill). Overall fuel cell system performance is summarized in Table 6, which indicates that the vehicle range is nearly 480 miles with an average efficiency of 75.6%. Consequently, in spite of the much greater mass of the fuel system compared with a conventional diesel engine, a comparable range is achieved with a high efficiency.

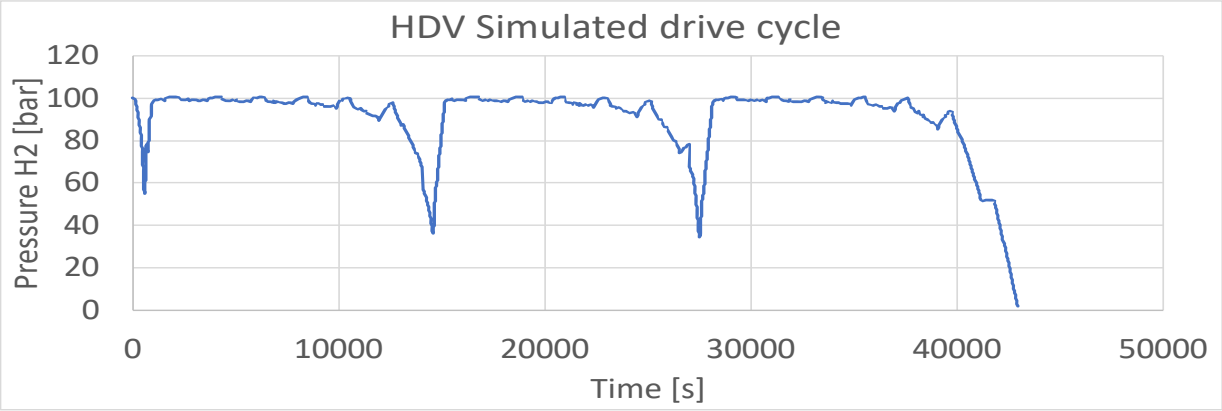

Figure 15. Vehicle Framework Model's HDV drive cycle results.

Table 6. Fuel cell system performance predicted by the combination of the MHSDT and Vehicle Framework models.

Usable H_2	60.35 kg
Distance travelled	478.6 miles
On-board efficiency	75.20%

2.3. Task 3 – Outreach

Communication of project results to the wider scientific community and to industry and utilities was accomplished in several ways.

2.3.1. Publications

Two manuscripts describing the results of this work aree in progress. We expect to be submitting the first one within the next one-to-two months and the second within four-to-five months:

1. M. Witman, V. Stavila, K. Brooks, M. D. Allendorf et al. "Co-design reveals the critical performance tradeoffs of metal-hydride nanoscaling and its necessity for a functional materials-based hydrogen storage system" *manuscript in preparation.*

2. M. Witman, V. Stavila, K. Brooks, L. Klebanoff, M. D. Allendorf "Materials and systems co-design reveals lithium magnesium amides as replacements for compressed gas in heavy duty transportation" *manuscript in preparation.*

2.3.2. Press release

Sandia will issue a press release; we plan this once the manuscripts have been submitted (even better would be to wait until they are published, but that will introduce too large a delay). We have contacts at scientific news organizations (e.g., *Chemistry World* and *Research Outreach*) and will plan interviews with them.

2.3.3. Presentations at scientific meetings

Support from SoCalGas was acknowledged in presentations at the following international scientific conferences and in several invited presentations at academic institutions:

1. M. D. Allendorf *International Symposium on Hydrogen & Energy*, Jan. 23, 2023
2. Invited seminar, Dept. of Chemistry, Colorado School of Mines, Golden, CO, Oct. 21, 2022.
3. Invited seminar, Institute of Materials Science and Engineering, Washington University in St. Louis, St. Louis, MO, Nov. 7, 2022.
4. V. Stavila et al. *MH-2022 Symposium on Metal-Hydrogen Systems, 2022*, Oct. 30 – Nov. 4, 2022, Perth, Australia.

2.3.4. Webinar

We presented a webinar entitled "Materials-Based Hydrogen Storage for Heavy Duty Vehicles" on Oct. 14, 2021, which was organized and delivered through SoCalGas.

2.3.5. Share results with DOE program managers

Our DOE program managers in the Hydrogen Fuel Cell Technologies Office have been informed about the project since its inception. We also acknowledged support by SoCalGas at the Hydrogen and Fuel Cells Program Annual Merit Review in 2021 and 2022 and will also do this at the 2023 AMR in June 2023.

3. CONCLUSION

3.1. Summary of key conclusions

The primary goal of this investigation was to assess whether a materials-based storage system for hydrogen could be a viable alternative to pressurized hydrogen gas. Although hydrogen storage as pressurized gas is a mature technology and fuel cell-powered vehicles, both HDV and LDV, are being designed employing it as the storage medium, it is clear that its limitations severely restrict fuel system design flexibility. Moreover, although this study did not explicitly consider the economics of the storage system, it is well known that Type IV fiber-reinforced tanks are costly,[30] as are 700-bar compressors and their maintenance.

Consequently, the highest-impact result of this study is the conclusion that it is indeed possible to design a hydrogen storage system based on a metal hydride that has volumetric capacity comparable to 700 bar pressurized gas and potentially even higher gravimetric storage capacity. These conclusions are based on the analysis we performed using measured properties of ($2LiNH_2$:$1MgH_2$:0.1KH:0.1LiH with 10 wt% SGL expanded graphite), a metal hydride/carbon composite with credible potential as a storage material compared not only with pressurized gas but also with other hydrides and liquid hydrogen. The attractive properties of this material, in addition to its storage capacity, are its composition of earth-abundant elements, high thermal conductivity and thermodynamics in the correct range to reduce heat management issues, and tailorable properties that can be leveraged to optimize performance for specific applications. In contrast, although there are many other metal hydrides that have been considered for on-board storage,[30] some of which are indicated in Figure 1, extensive research by HyMARC and others has identified aspects that make some of these impractical for transportation applications. These problems include poor reversibility (e.g. $Mg(BH_4)_2$),[35, 36] sluggish release kinetics (complex hydrides such as $NaAlH_4$), low gravimetric capacity, as in interstitial and intermetallic hydrides,[30] and metastability (e.g. AlH_3).[37] The comparison of the 2:1 material with liquified hydrogen is also favorable. Aside from the attendant cryogenic issues associated with storing liquid hydrogen, its usable capacity is significantly reduced by the fact that 35% of its energy is required for liquification, which is triple the energy required to compress the gas to 700 bar.[30]

A second key result obtained from our analysis is that there appear to be alternatives to conventional materials used to fabricate high-pressure hydrogen tanks (primarily 316 SS and carbon fiber-reinforced plastic). We considered a total of twelve alloys and found that tanks fabricated from several of these have material specifications compatible with the temperatures needed to dehydrogenate the 2:1 material and are also light enough to provide the necessary gravimetric and volumetric system capacities. However, the suitability of these alloys for on-board hydrogen storage must still be established. Although the maximum pressure required to regenerate the 2:1 material is relatively low compared with pressurized gas (100 bar vs. 350 or 700 bar), it could cause hydrogen embrittlement in some materials. Consequently, metallurgical investigations must be conducted where data are lacking to establish the durability and safety of these alloys for hydrogen storage.

3.2. *Next steps*

The results of our investigation are promising and motivate additional research to increase its TRL, which we conservatively designate as TRL 3. Specific areas where additional R&D are needed (in order of priority) include the following. Areas (1) and (2) are the logical next steps for HDV in our opinion.

1. Given that our analysis shows that the lithium-magnesium amide/graphite composite material

has the properties required to store hydrogen efficiently onboard a HDV and operate its fuel cell, a logical next step is to perform a techno-economic analysis (TEA) to assess its economic viability. TEA of other storage materials such as MOFs have been reported for bulk hydrogen transport[38] and for LOHC[39] but not for on-board storage to operate a HDV-FCEV. For metal hydrides, a TEA of refueling station costs is encouraging, estimating that station costs for using a metal hydride are 39% lower than for storing hydrogen as a. gas at 700 bar.[40] These savings are largely due to the lower cost of the 100 bar compressor required to refuel the vehicle (i.e., to regenerate the metal hydride).

2. Long-term cycling tests under simulated HDV conditions; these are needed to demonstrate long-term reversibility and preservation of storage capacity.
3. Refueling process: regeneration of these metal hydrides has different kinetics from the hydrogen release process. A co-design process that takes into consideration both fuel system design and refueling in the context of the various HDV use cases is a logical next step.
4. Consideration of hydrides of various types for point-of-delivery for storage: large amounts of hydrogen must be stored at refueling stations, where system mass and volume are less of a consideration than for on-board applications. In this case, materials such as intermetallic hydrides could be an economical solution and avoid the need for high-pressure compression at the fueling station.
5. Beyond bench-scale experiments: Research to date has concentrated on laboratory-scale measurements, which of necessity involve very small quantities (at most a few grams) of material. Scaling up the synthesis to produce larger quantities needed for small-scale demonstration projects (up to 1 kg of material) is needed.

REFERENCES

1. Target Explanation Document: Onboard Hydrogen Storage for Light-Duty Fuel Cell Vehicles. https://www.energy.gov/eere/fuelcells/downloads/target-explanation-document-onboard-hydrogen-storage-light-duty-fuel-cell.
2. Ahluwalia, R. K.; Huaa, T. Q.; Peng, J. K.; Lasher, S.; McKenney, K.; Sinha, J.; Gardiner, M., Technical assessment of cryo-compressed hydrogen storage tank systems for automotive applications. *International Journal of Hydrogen Energy* **2010,** *35* (9), 4171-4184.
3. Petitpas, G.; Aceves, S., Hydrogen Storage in Pressure Vessels: Liquid, Cryogenic, and Compressed Gas. In *Hydrogen Storage Technology, Materials and Applications*, Klebanoff, L. E., Ed. Taylor and Francis: Boca Raton, 2012; p 97.
4. Laughlin, M.; Burnham, A. *Case Study: Natural-Gas-Fueled Regional Transport Trucks*; U.S. Department of Energy: August 2016, 2016.
5. Allendorf, M. D.; Stavila, V.; Snider, J. L.; Witman, M.; Bowden, M. E.; Brooks, K.; Tran, B. L.; Autrey, T., Challenges to developing materials for the transport and storage of hydrogen. *Nat. Chem.* **2022,** *14* (11), 1214-1223.
6. Bogdanović, B.; Schwickardi, M., Ti-doped alkali metal aluminium hydrides as potential novel reversible hydrogen storage materials1Invited paper presented at the International Symposium on Metal–Hydrogen Systems, Les Diablerets, August 25–30, 1996, Switzerland.1. *Journal of Alloys and Compounds* **1997,** *253-254*, 1-9.
7. Garroni, S.; Santoru, A.; Cao, H. J.; Dornheim, M.; Klassen, T.; Milanese, C.; Gennari, F.; Pistidda, C., Recent Progress and New Perspectives on Metal Amide and Imide Systems for Solid-State Hydrogen Storage. *Energies* **2018,** *11* (5).
8. Chen, P.; Xiong, Z.; Luo, J.; Lin, J.; Tan, K. L., Interaction of hydrogen with metal nitrides and imides. *Nature* **2002,** *420* (6913), 302-304.
9. Wood, B. C.; Stavila, V.; Poonyayant, N.; Heo, T. W.; Ray, K. G.; Klebanoff, L. E.; Udovic, T. J.; Lee, J. R. I.; Angboonpong, N.; Sugar, J. D.; Pakawatpanurut, P., Nanointerface-Driven Reversible Hydrogen Storage in the Nanoconfined Li–N–H System. *Advanced Materials Interfaces* **2017,** *4* (3), 1600803.
10. Stavila, V.; Klebanoff, L. Nanostructured Metal Amides and Nitrides for Hydrogen Storage. 10000377, 2018.
11. Luo, W., (LiNH2–MgH2): a viable hydrogen storage system. *Journal of Alloys and Compounds* **2004,** *381* (1), 284-287.
12. Xiong, Z.; Wu, G.; Hu, J.; Chen, P., Ternary Imides for Hydrogen Storage. *Advanced Materials* **2004,** *16* (17), 1522-1525.
13. Dedrick, D. E.; Kanouff, M. P.; Replogle, B. C.; Gross, K. J., Thermal properties characterization of sodium alanates. *Journal of Alloys and Compounds* **2005,** *389* (1), 299-305.
14. Johnson, T. A.; Kanouff, M. P.; Dedrick, D. E.; Evans, G. H.; Jorgensen, S. W., Model-based design of an automotive-scale, metal hydride hydrogen storage system. *International Journal of Hydrogen Energy* **2012,** *37* (3), 2835-2849.
15. Chen, P.; Zhu, M., Recent progress in hydrogen storage. *Materials Today* **2008,** *11* (12), 36-43.
16. Li, C.; Fan, M. Q.; Chen, H. C.; Chen, D.; Tian, G. L.; Shu, K. Y., Thermodynamics and Kinetics Modifications on the Li-Mg-N-H Hydrogen Storage System. *Progress in Chemistry* **2016,** *28* (12), 1788-1797.
17. Qin, D. L.; Zhao, X. Y.; Zhang, K.; Lu, J.; Zhang, H. B.; Xin, S. G., Effects of Composition on Hydrogen Storage Properties of Li-Mg-N-H System. *Rare Metal Materials and Engineering* **2015,** *44* (2), 355-359.
18. Tokoyoda, K.; Ichikawa, T.; Miyaoka, H., Evaluation of the enthalpy change due to hydrogen

desorption for M-N-H (M = Li, Mg, Ca) systems by differential scanning calorimetry. *International Journal of Hydrogen Energy* **2015,** *40* (3), 1516-1522.
19. NIST Chemistry WebBook. https://webbook.nist.gov/chemistry/). (accessed accessed 12 August, 2022).
20. Wang, J.; Liu, T.; Wu, G.; Li, W.; Liu, Y.; Araújo, C. M.; Scheicher, R. H.; Blomqvist, A.; Ahuja, R.; Xiong, Z.; Yang, P.; Gao, M.; Pan, H.; Chen, P., Potassium-Modified Mg(NH2)2/2 LiH System for Hydrogen Storage. *Angewandte Chemie International Edition* **2009,** *48* (32), 5828-5832.
21. Osborne, D. W.; Flotow, H. E., Lithium nitride (Li3N): heat capacity from 5 to 350 K and thermochemical properties to 1086 K. *The Journal of Chemical Thermodynamics* **1978,** *10* (7), 675-682.
22. Gross, K. J.; Carrington, K. R.; Barcelo, S.; Karkamkar, A.; Purewal, J. Recommended Best Practices for the Characterization of Storage Properties of Hydrogen Storage Materials. https://www.energy.gov/eere/fuelcells/articles/recommended-best-practices-characterization-storage-properties-hydrogen-0 (accessed June 26, 2023).
23. Bhakta, R. K.; Maharrey, S.; Stavila, V.; Highley, A.; Alam, T.; Majzoub, E.; Allendorf, M., Thermodynamics and kinetics of $NaAlH_4$ nanocluster decomposition. *Physical Chemistry Chemical Physics* **2012,** *14* (22), 8160-8169.
24. Hydrogen Materials Advanced Research Consortium: Hydrogen Storage Systems Modeling. https://www.hymarc.org/models.html.
25. Klymyshyn, N. A.; Barrett, N. P. *PNNL Tank Mass Estimator for Cross Comparison of Type 1, Type 3, and Type 4 Pressure Vessels ("Tankinator")*; PNNL-SA-179141; Pacific Northwest National Laboratory: Richland, WA, 2022.
26. Sprik, S.; Brooks, K.; Grady, C.; Thornton, M. Hydrogen Storage System Modeling: Public Access, Maintenance, and Enhancements. https://www.hydrogen.energy.gov/pdfs/review22/st008_thornton_2022_p.pdf.
27. Hydrogen Storage Engineering Center of Excellence. https://www.energy.gov/eere/fuelcells/hydrogen-storage-engineering-center-excellence (accessed Feb. 7, 2023).
28. Motyka, T. *Hydrogen Storage Engineering Center of Excellence Metal Hydride Final Report*; 2014, Savannah River National Laboratory Report, 2014, SRNL-STI-2014-00226, DOI 10.2172/1171992.
29. Brooks, K. P.; Sprik, S. J.; Tamburello, D. A.; Thornton, M. J., Design tool for estimating metal hydride storage system characteristics for light-duty hydrogen fuel cell vehicles. *International Journal of Hydrogen Energy* **2020,** *45* (46), 24917-24927.
30. Durbin, D. J.; Malardier-Jugroot, C., Review of hydrogen storage techniques for on board vehicle applications. *International Journal of Hydrogen Energy* **2013,** *38* (34), 14595-14617.
31. Li, J.; Liu, J.; Zhao, B.; Wang, D.; Guo, S.; Song, J.; Li, X., Research on Temperature Rise of Type IV Composite Hydrogen Storage Cylinders in Hydrogen Fast-Filling Process. *Energies* **2023,** *16* (6), 2918.
32. Corgnale, C.; Hardy, B. J.; Tamburello, D. A.; Garrison, S. L.; Anton, D. L., Acceptability envelope for metal hydride-based hydrogen storage systems. *International Journal of Hydrogen Energy* **2012,** *37* (3), 2812-2824.
33. Witman, M.; Ling, S.; Wadge, M.; Bouzidi, A.; Pineda-Romero, N.; Clulow, R.; Ek, G.; Chames, J.; Allendorf, E.; Agarwal, S.; Allendorf, M.; Walker, G.; Grant, D.; Sahlberg, M.; Zlotea, C.; Stavila, V., Towards Pareto optimal high entropy hydrides via data-driven materials discovery. *ChemRxiv* **2022**.
34. NREL DriveCAT - Chassis Dynamometer Drive Cycles. (2023). www.nrel.gov/transportation/drive-cycle-tool (accessed March 15, 2023).

35. Ray, K. G.; Klebanoff, L. E.; Lee, J. R. I.; Stavila, V.; Heo, T. W.; Shea, P.; Baker, A. A.; Kang, S.; Bagge-Hansen, M.; Liu, Y.-S.; White, J. L.; Wood, B. C., Elucidating the mechanism of MgB2 initial hydrogenation via a combined experimental–theoretical study. *Physical Chemistry Chemical Physics* **2017,** *19* (34), 22646-22658.
36. Zavorotynska, O.; El-Kharbachi, A.; Deledda, S.; Hauback, B. C., Recent progress in magnesium borohydride Mg(BH4)2: Fundamentals and applications for energy storage. *International Journal of Hydrogen Energy* **2016,** *41* (32), 14387-14403.
37. Graetz, J.; Reilly, J. J., Kinetically stabilized hydrogen storage materials. *Scripta Materialia* **2007,** *56* (10), 835-839.
38. Anastasopoulou, A.; Furukawa, H.; Barnett, B. R.; Jiang, H. Z. H.; Long, J. R.; Breunig, H. M., Technoeconomic analysis of metal-organic frameworks for bulk hydrogen transportation. *Energy & Environmental Science* **2021,** *14* (3), 1083-1094.
39. Niermann, M.; Drunert, S.; Kaltschmitt, M.; Bonhoff, K., Liquid organic hydrogen carriers (LOHCs) - techno-economic analysis of LOHCs in a defined process chain. *Energy & Environmental Science* **2019,** *12* (1), 290-307.
40. Frank, E. D.; Elgowainy, A.; Khalid, Y. S.; Peng, J. K.; Reddi, K., Refueling-station costs for metal hydride storage tanks on board hydrogen fuel cell vehicles. *International Journal of Hydrogen Energy* **2019,** *44* (57), 29849-29861.

APPENDIX 1. MHSDT MODEL PREDICTIONS OF STORAGE SYSTEM PROPERTIES FOR PRESSURIZED GAS

	Light Duty Vehicle (5.6 kg)		Heavy Duty Vehicle (60 kg)		
	350 Bar	700 Bar	350 Bar	700 Bar	Units
H_2 Gas Volumetric Density	23.696	38.73	23.696	38.73	g/L @ 20°C, gas only
Tank Internal Volume	236	145	2532	1549	Liters & 20 cm diameter
Total H_2	5600	5600	60000	60000	g
Tank Internal Length	2	2	2	2	m
Number of Tanks	2	2	8	4	
Calculated Internal Diameter	0.28	0.22	0.46	0.52	m
Volume Tank--Tankinator Carbon Fiber	294	219	3147	2386	L (Type III, Low Bound)
Volume Tank--Tankinator 316 SS	351	390	3816	4456	L
Volume Tank--Tankinator Al 6061	430	748	4720	9000	L
Volume Tank--Tankinator A286	274	200	2944	2180	L
System Volumetric Density Carbon Fiber	19.0	25.5	19.1	25.1	g/L system
System Volumetric Density 316 SS	16.0	14.4	15.7	13.5	g/L system
System Volumetric Density Al 6061	13.0	7.5	12.7	6.7	g/L system
System Volumetric Density A286	20.5	28.0	20.4	27.5	g/L system
2025 Volumetric Target	40	40	N/A	N/A	g/L
Percent of 2025 Volumetric Target Carbon Fiber	48%	64%	N/A	N/A	%
Percent of 2025 Volumetric Target 316 SS	40%	36%	N/A	N/A	%
Percent of 2025 Volumetric Target Al 6061	33%	19%	N/A	N/A	%
Percent of 2025 Volumetric Target A286	51%	70%	N/A	N/A	%
Mass Tank--Tankinator Carbon Fiber	123	157	1332	1766	kg
Mass Tank--Tankinator 316 SS	932	1978	10424	23404	kg
Mass Tank--Tankinator Al 6061	520	1610	5860	19868	kg
Mass Tank--Tankinator A286	307	443	3416	5068	kg
System Gravimetric Density Carbon Fiber	0.045	0.036	0.045	0.034	kg H2/kg system
System Gravimetric Density 316 SS	0.006	0.003	0.006	0.003	kg H2/kg system
System Gravimetric Density Al 6061	0.011	0.003	0.010	0.003	kg H2/kg system
System Gravimetric Density A286	0.018	0.013	0.018	0.012	kg H2/kg system

2025 Gravimetric Target	0.055	0.055	N/A	N/A	kg H2/kg system
Percent of 2025 Gravimetric Target Carbon Fiber	83%	65%	N/A	N/A	%
Percent of 2025 Gravimetric Target 316 SS	11%	5%	N/A	N/A	%
Percent of 2025 Gravimetric Target Al 6061	20%	6%	N/A	N/A	%
Percent of 2025 Gravimetric Target A286	33%	23%	N/A	N/A	%

DISTRIBUTION

Email—Internal

Name	Org.	Sandia Email Address
Kristin Hertz	8367	klhertz@sandia.gov
Christian Mailhiot	8340	cmailhi@sandia.gov
Richard A. Karnesky	8341	rakarne@sandia.gov
Vitalie Stavila	8341	vnstavi@sandia.gov
Matthew D. Witman	8341	mwitman@sandia.gov
Robert Horton	8367	rdhort@sandia.gov
Lennie E. Klebanoff	8367	lekleba@sandia.gov
Technical Library	1911	sanddocs@sandia.gov

Email—External

Name	Company Email Address	Company Name
Jeffrey P. Chase	JChase@socalgas.com	SoCalGas

This page left blank

Sandia National Laboratories

Sandia National Laboratories is a multimission laboratory managed and operated by National Technology & Engineering Solutions of Sandia LLC, a wholly owned subsidiary of Honeywell International Inc. for the U.S. Department of Energy's National Nuclear Security Administration under contract DE-NA0003525.